

Modeling the activation of small molecules and ions at biological
metal centers

(Summary)

By

Amr Ali Attia

A thesis submitted to the department of chemistry
in partial fulfillment of the requirements for the degree of

Doctor of Philosophy

in

Chemistry

Scientific advisor: Assoc. Prof. Dr. Radu Silaghi-Dumitrescu

Babeş-Bolyai University

Cluj-Napoca, Romania

Modeling the activation of small molecules and ions at biological
metal centers

(Summary)

By

Amr Ali Attia

Babeş-Bolyai University

Cluj-Napoca, Romania

Jury

President:

Prof. Dr. Mircea Diudea

Babeş-Bolyai University

Reviewers:

Conf. Dr. Gabriela Nemeş

Prof. Dr. Ionel Humelnicu

CŞII Dr. Attila Bende

Babeş-Bolyai University

AI Cuza University of Iaşi

I.N.C.D.T.I.M. Cluj-Napoca

Contents

Abstract	6
Part I: Dioxygen binding and activation	9
1. Superoxide reductase	10
1.1. Introduction	10
1.2. Theoretical methods	15
1.3. Results and discussions	17
1.3.1. Fe–O vs. O–O bond cleavage in reactive iron peroxide intermediates of SOR	17
1.3.2. The electronic structure of $\{\text{FeO}_2\}^9$ at the DFT, MP2 and MC-CASSCF levels	24
1.4. Conclusions	29
1.5. References	29
2. Oxygen transporters: Beyond the usual suspects	33
2.1. Introduction	33
2.2. Theoretical methods	36
2.3. Results and discussions	37
2.3.1. Hemoglobin and CYP ₄₅₀	37
2.3.2. Hemerythrin	51
2.3.3. Mononuclear non-heme iron complexes (NHFe)	55
2.4. Conclusions	61
2.5. References	62
3. The reaction mechanism of cysteine dioxygenase.	65
3.1. Introduction	65
3.2. Theoretical methods	66

3.3. Results and discussions	68
3.4. Conclusions	78
3.5. References	79
Part II: Nitric oxide binding and reduction	81
4. The binding and reduction of NO at the active site of SOR	82
4.1. Introduction	82
4.2. Theoretical methods	83
4.3. Results and discussions	84
4.3.1. The electronic structure of {FeNO} ⁷ SOR-nitrosyl complex at the DFT and MP2 levels	84
4.3.2. The electronic structure of {FeNO} ⁷ SOR-nitrosyl complex at the CASSCF level	88
4.4. Conclusions	92
4.5. References	93
5. The Super-reduced mechanism of nitric oxide reduction in flavo-diiron NO reductases	97
5.1. Introduction	97
5.2. Theoretical methods	98
5.3. Results and discussions	100
5.4. Conclusions	106
5.5. References	106
6. Bacterial nitric oxide reductase: A mechanism revisited by an ONIOM (DFT:MM) study.	108
6.1. Introduction	108
6.2. Theoretical methods	110
6.3. Results and discussions	112
6.4. Conclusions	125
6.5. References	126

7. Asymmetry within the iron dinitrosyl moiety of dithiolate dinitrosyl iron complexes	129
7.1. Introduction	129
7.2. Theoretical methods	132
7.3. Results and discussions	137
7.3.1 Excited states vs. ground state in DNIC models	137
7.3.2 The electronic structure of $\{\text{Fe}(\text{NO})_2\}^9$ at the CASSCF level	142
7.3.3 Ab initio molecular dynamics calculations	143
7.3.4 Reaction pathways leading to the formation of nitrogen-nitrogen bonds	146
7.4. Conclusions	148
7.5. References	149
Part III: Nitrogen oxianions	154
8. A theoretical study on the reaction pathways of peroxyxynitrite formation and decay at <i>non</i>-heme iron centers	155
8.1. Introduction	155
8.2. Theoretical methods	158
8.3. Results and discussions	160
8.3.1. Coordination of the anion OONO^-	160
8.3.2. Coordination of ONOOH	170
8.4. Conclusions	178
8.5. References	179
9. Computational investigation of the initial two-electron, two-proton steps in the reaction mechanism of hydroxylamine oxidoreductase	183
9.1. Introduction	183
9.2. Theoretical methods	184
9.3. Results and discussions	185
9.4. Conclusions	192
9.5. References	192

Summary	195
Acknowledgments	200
Appendix A: Supporting information	201
Appendix B: Publications	258

Abstract

The computational and theoretical results presented in this thesis provide new advancements in several active areas of research in the field of bioinorganic chemistry. The topics investigated in this thesis span over a total of nine chapters. Each chapter represents a duly adapted version of a published paper or a manuscript submitted (or about to be submitted) to a journal by the candidate - with a number of 9 papers/manuscripts. The first part of the thesis deals with dioxygen binding and activation and is comprised of three chapters covering the mechanism of superoxide reduction at the active site of superoxide reductase, the reversible dioxygen binding mechanism at the active sites of heme and non-heme enzymes, and the mechanism of cysteine oxidation by nickel cysteine dioxygenase. Part II features nitric oxide binding and reduction and is structured into four chapters, addressing the binding of nitric oxide to the active site of superoxide reductase, the reduction of nitric oxide and the generation of nitrous oxide at the active sites of flavo-diiron nitric oxide reductase and bacterial nitric oxide reductase, together with a discussion on nitric oxide donation and the structural asymmetries of biologically relevant dithiolate dinitrosyl iron complexes. The third part of this thesis covers nitrogen oxyanions and presents an investigation of the formation and decomposition of peroxyxynitrite at the active sites of superoxide reductase and superoxide dismutase and lastly, the mechanism of hydroxylamine oxidation at the active site of hydroxylamine oxidoreductase.

Keywords: iron, non-heme, superoxide, superoxide reductase, SOR, DFT, CASSCF, dioxygen, heme, redox, myoglobin, hemoglobin, hemerythrin, MNFe, cysteine dioxygenase, CDO, nickel, nitric oxide, flavo-diiron, nitric oxide reductase, cNOR, ONIOM, dinitrosyl, DNICs, peroxyxynitrite, superoxide dismutase, SOD, hydroxylamine oxidoreductase, HAO, electron/proton affinity.

In the present thesis, quantum chemical computations at multiple levels of theory were successfully applied to various biological metal systems. The results obtained provided considerable developments to currently active research areas in the field of bioinorganic chemistry.

The first part of this thesis dealt with dioxygen binding and activation and incorporated three chapters.

Chapter 1. Superoxide reductases.

Chapter 1 investigated the reduction of superoxide at the active site of the superoxide scavenging enzyme superoxide reductase. Meta hybrid DFT (Mo6-2X) results for the reactivity of the putative peroxy/hydroperoxy reaction intermediates in the catalytic cycle of SORs were found to indicate a high-spin preference in all cases. An exploration of the energy profiles for Fe–O and O–O bond cleavage in all spin states in both ferric and ferrous models revealed that Fe–O bond cleavage always occurred more easily than O–O bond cleavage. O–O bond cleavage appeared to be thermodynamically and kinetically unfeasible in ferric hydrogen peroxide complexes whereas it was proposed to occur as a minor (significantly disfavored) side reaction in the interaction of ferrous SOR with hydrogen peroxide. [1,2]

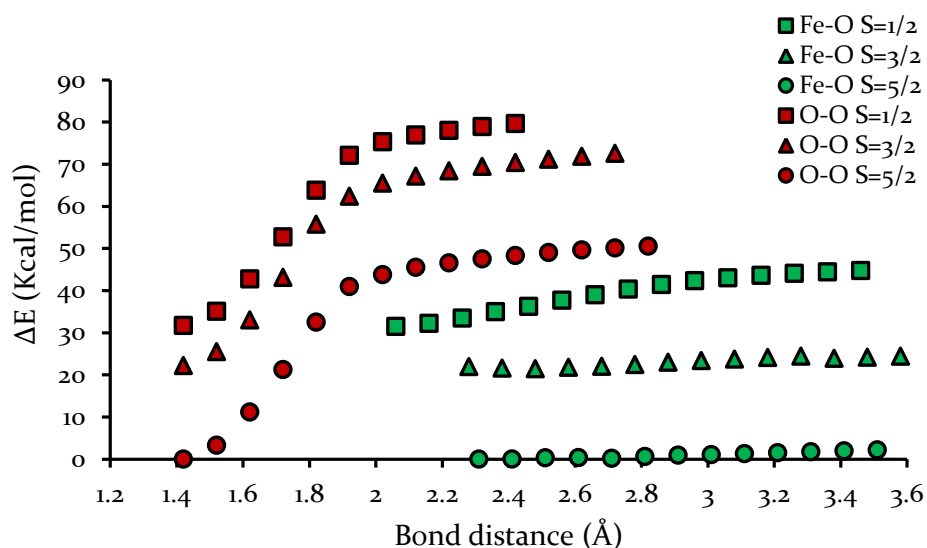


Figure 1.1. Energy profiles of Fe–O and O–O for a putative ferric hydrogen peroxide SOR reaction intermediate; the equilibrium energy of the high-spin state was taken as an arbitrary reference.

Multiconfigurational CASSCF results on the $\{\text{FeO}_2\}^9$ (formally ferrous-superoxo) structure of SOR revealed an electronic structure with a highly covalent interaction between Fe and the dioxygenic ligand. An attempt to separate the strongly interacting orbitals by a Cholesky decomposition localization procedure [3] was carried out and the resulting principal configuration comprised the Fe(III)-O_2^{2-} and the Fe(II)-O_2^- resonance structures with a contribution of about 82% to the total weight of the wave function. [1,2]

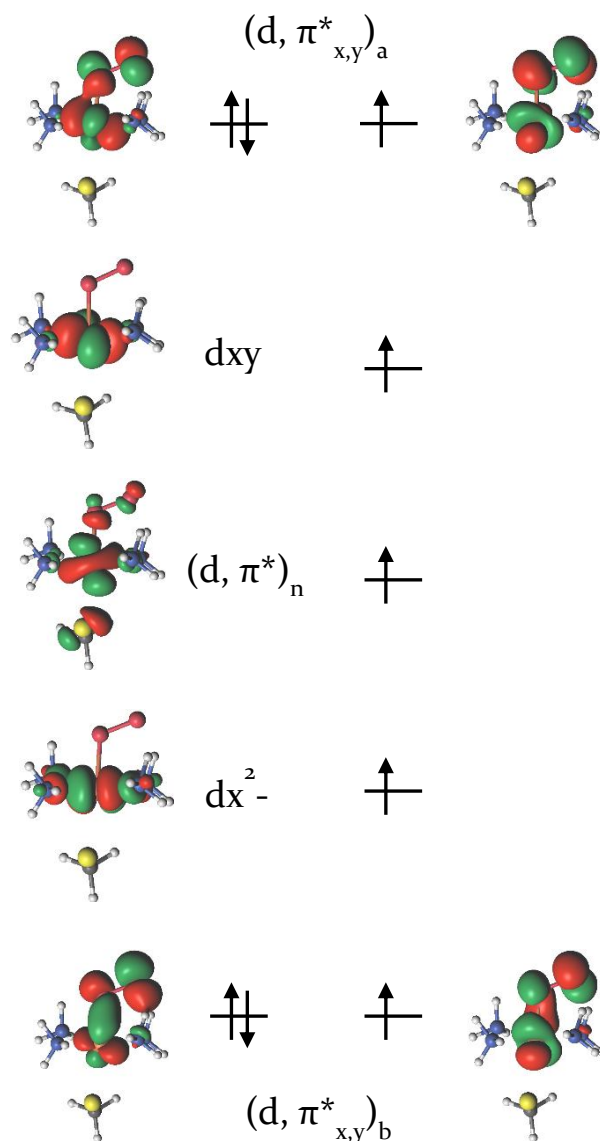


Figure 1.2. CASSCF natural orbitals and principal electronic configurations of the $\{\text{FeO}_2\}^9$ SOR structure.

Chapter 2. Oxygen transporters.

The reversible binding mechanism of the dioxygenic ligand at iron centers of heme (hemoglobin and cytochrome P450 mono-oxygenase), binuclear non-heme (hemerythrin), and mono-nuclear non-heme enzymes was studied in chapter 2. The electronic structures of oxy- and aqua-bound active sites of heme (Hb, CYP450) iron systems were studied by pure, hybrid and meta hybrid GGA DFT functionals. The singlet ground state of oxyhemoglobin was only reproducible within the framework of the broken symmetry approach. The potential energy profiles for Fe–O bond cleavage revealed a significant effect of the functional in describing the reversible binding mechanism of the dioxygenic ligand which appeared anywhere from facile to impossible, depending on the functional employed. The pitfalls of each of the functionals employed were analyzed, thus allowing one to better avoid over interpretation of DFT-derived data on the reactivity and spin state preference in bioinorganic systems. [4]

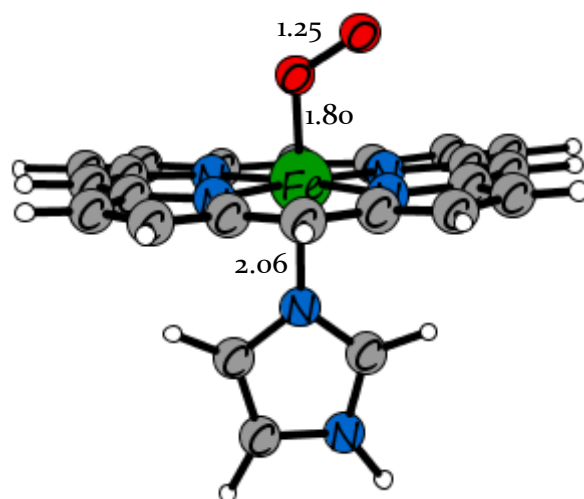


Figure 2.1. The optimized structure of the oxyhemoglobin complex in the ground state as computed by the Mo6-L functional.

The results discussed in this chapter revealed some unique characteristics that contribute to the efficiency of hemoglobin and hemerythrin in the reversible dioxygen binding mechanism. These traits range from low spin induction (by coupling antiferromagnetically to dioxygen) and the ability of spin crossing in hemoglobin to

diiron antiferromagnetic coupling and the conversion of dioxygen to a hydroperoxo by a proton coupled 2-electron transfer process in hemerythrin. [5,6]

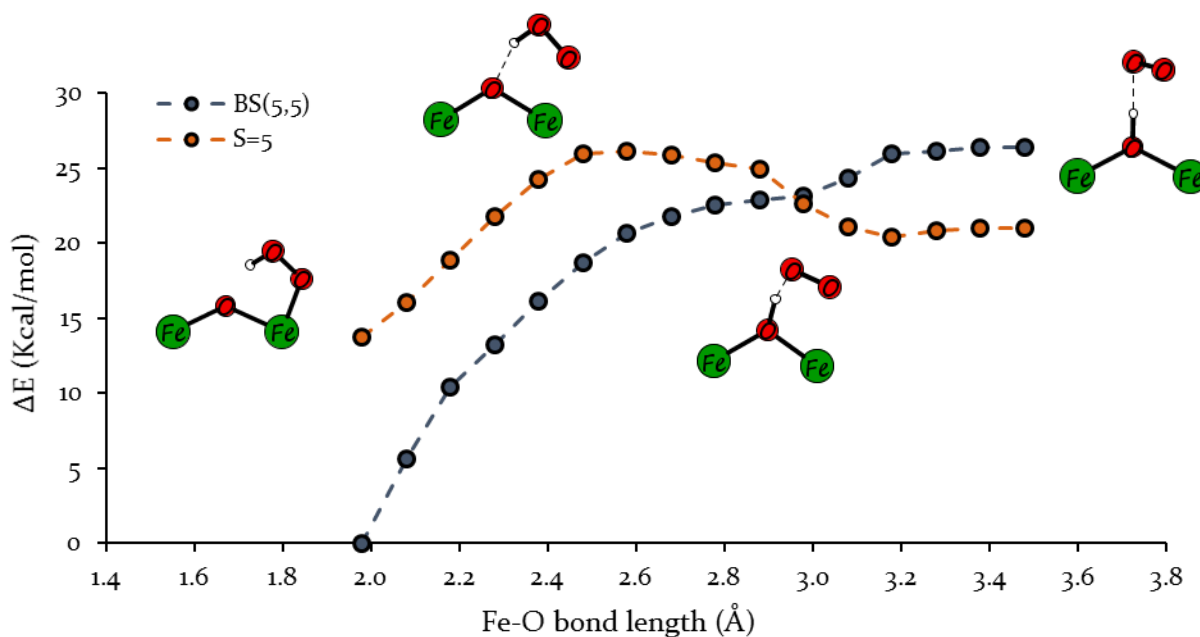


Figure 2.2. Potential energy profile for Fe-O bond cleavage in oxy-hemerythrin as computed by Mo6-L.

On the other hand, none of these traits were noticed in the NHFe structures; the high spin ground states showed no tendency for stable reversible dioxygen binding and, when coupled with the peroxo description of the dissociated dioxygen, renders the NHFe complexes as very poor choice for dioxygen transportation.

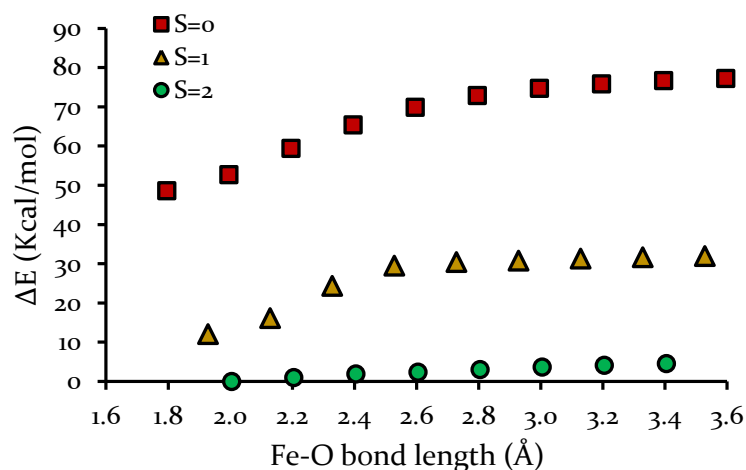


Figure 2.3. Potential energy profile for Fe-O bond cleavage in SOR-dioxygen computed by Mo6-L.

Chapter 3. The reaction mechanism of nickel cysteine dioxygenase.

Chapter 3 focused on the reaction mechanism as well as the reactive intermediates involved in the catalytic cycle of nickel cysteine dioxygenase - a 3-His ligated non-heme enzyme involved in the catalytic metabolism of cysteine. [7]

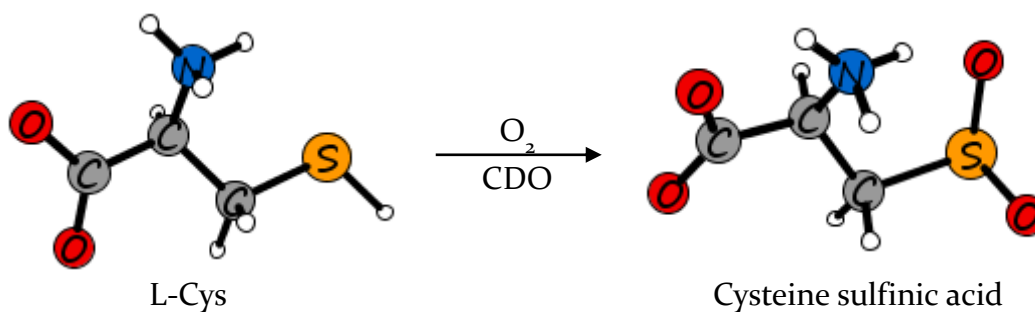


Figure 3.1. CDO catalyzes the oxidation of L-Cys to cysteine sulfinic acid.

DFT results showed that the starting structure of the reaction mechanism featured an octahedral Ni(III)-superoxo active site with cysteine substrate binding in a bidentate fashion. A stepwise transfer of the oxygen atoms of superoxide to the sulfur atom of the bound cysteine substrate took place to form a sulfenate intermediate followed by cysteine sulfinic acid.

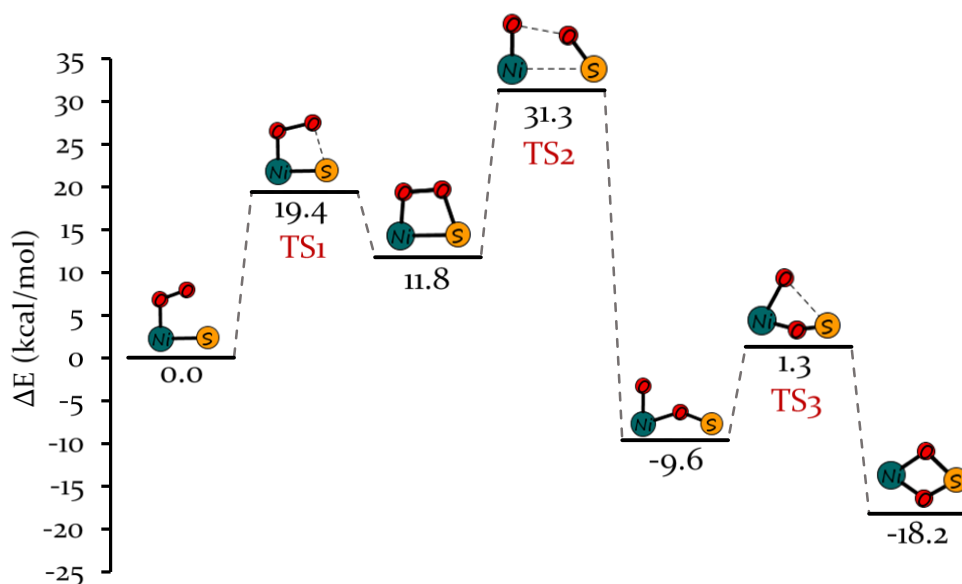


Figure 3.2. The potential energy profile for the dioxygenation of cysteine by Ni CDO.

The O-O bond breaking to yield the sulfenate intermediate was found to be the rate limiting step with an energy barrier of almost 20 kcal/mol. This step was shown to lead to a somewhat unusual $S=2$ Ni(IV)-oxo center. The overall reaction mechanism as well as the nature of the catalytic intermediates were found to be similar to those reported for iron CDOs; however, the energy barriers along the potential energy surface of the reaction were much higher - which supports the experimental findings that associate iron (as the active site metal ion) with increased catalytic activity.[8]

Part II of this thesis covered the binding and reduction of nitric oxide and constituted four chapters.

Chapter 4. The binding and reduction of NO at the active site of SOR.

In Chapter 4, the electronic structure of the nitrosyl-bound *non-heme* SOR iron complex was investigated with pure, hybrid and meta-hybrid GGA DFT functionals as well as the post Hartree-Fock MP2 and the multireference CASSCF levels of theory.

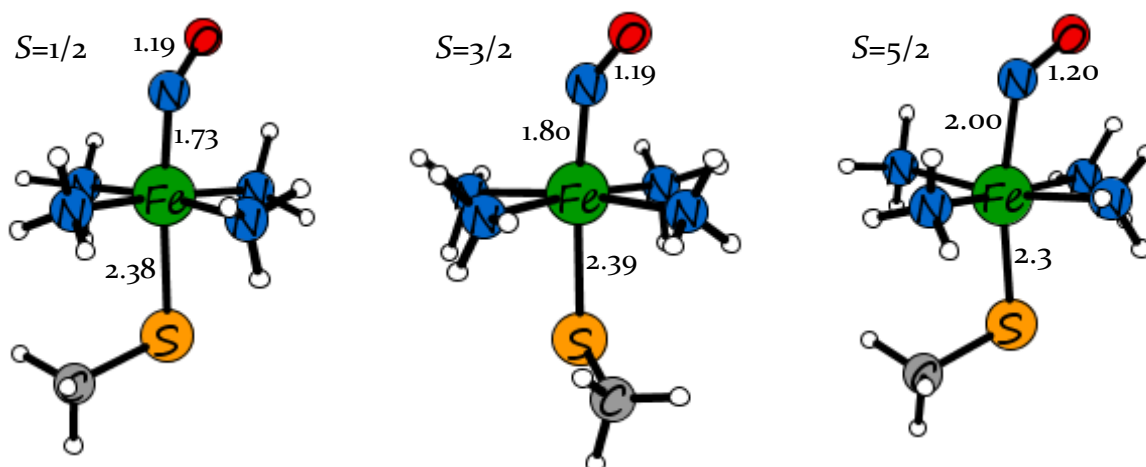


Figure 4.1. Optimized structures of the SOR-nitrosyl complex in all spin states as predicted by the Mo6-L DFT functional.

Several DFT functionals, namely Mo6-L, Mo6 and B3LYP, were shown to provide ground states and geometrical parameters that agree well with previously reported experimental and theoretical studies; the Mo6-L functional, however, stood out as the only functional capable of describing the antiferromagnetic coupling between Fe and NO as well as providing an anionic description of NO in contrast to a radical neutral NO predicted by the rest of the functionals. The post Hartree-Fock MP2 method provided an overall poor performance with unreasonable energies and unphysical geometries [4]. The analysis of the CASSCF wave function showed a highly covalent interaction and a bonding that is characterized by a strong antiferromagnetism between the Fe and NO fragments. In terms of localized orbitals obtained from a Cholesky decomposition procedure, the SOR-nitrosyl complex was best characterized as a mixture of Fe(II)-NO^o and Fe(III)-NO⁻ resonance structures. Potential energy profiles computed for cleaving the Fe-N and N-O bonds provided further insight into the instability of the SOR-nitrosyl complex.

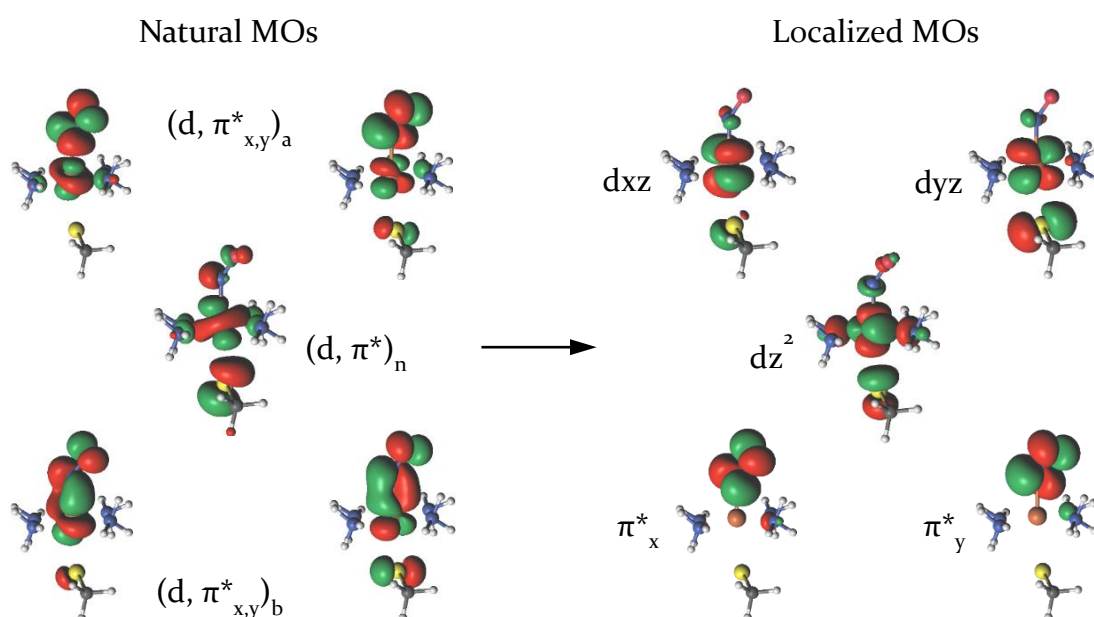


Figure 4.2. Natural MOs vs. Localized MOs as a product of Cholesky localization procedure.

Chaper 5. The Super-reduced mechanism of nitric oxide reduction in flavo-diiron NO reductases.

The key intermediates in the super-reduced diiron-dinitrosyl mechanism of NO reduction in FNORs were inspected in chapter 5 by means of density functional theory. The instant formation of a hyponitrite adduct upon the two-electron reduction of $[\{\text{FeNO}\}^7]_2$ was strongly suggested as the reaction initiator. Breaking the N-O bond of hyponitrite to yield N_2O was found to feature the highest energy barrier thus proposed to be the rate-limiting step. The potential energy profile obtained from the calculated intermediates was found to compete well with the previously proposed cis mechanism and provided an insight toward the feasibility of the super-reduced mechanism for NO reduction and N_2O generation by FNORs.[9,10]

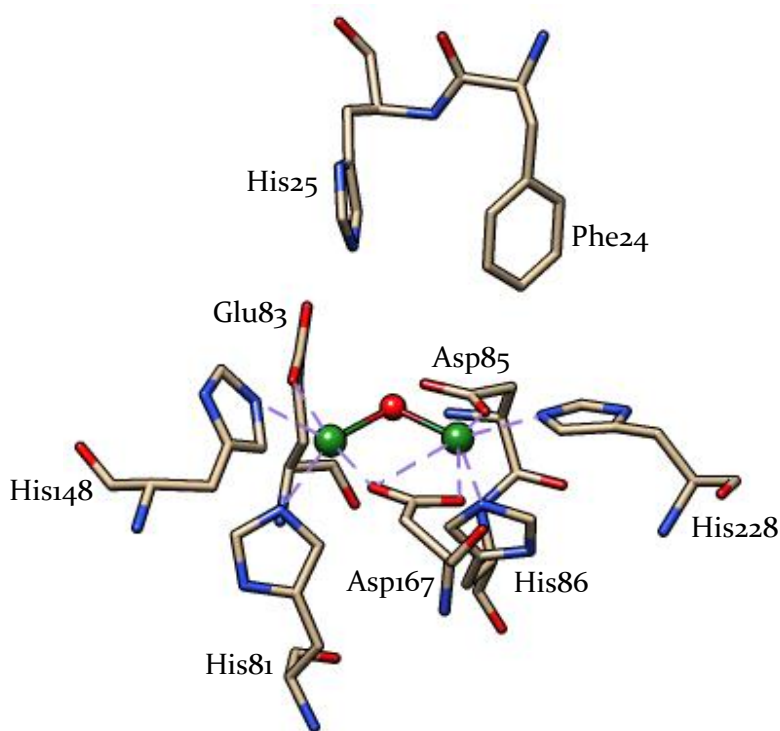


Figure 5.1. The active site and proximal key residues of flavo diiron NO reductase from the X-ray crystal structure of *Moorella thermoacetica* (pdb id 1ycg).

Chapter 6. Bacterial nitric oxide reductase: A mechanism revisited by an ONIOM (DFT:MM) study.

Chapter 6 featured an ONIOM (DFT:MM) study on the reaction mechanism of bacterial nitric oxide reductase (cNOR) to identify the possible reactive intermediates of the reaction. [11]

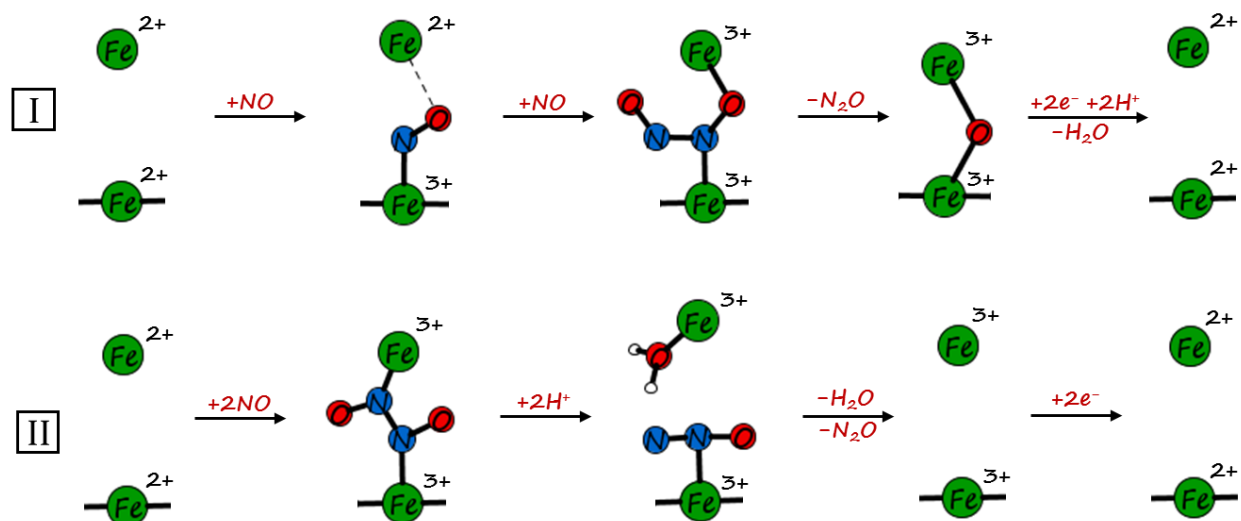


Figure 6.1. Proposed mechanisms for NO reduction by cNOR. (I) represents the cis Fe_{b3} mechanism while (II) represents the trans (dinitrosyl) mechanism.

The results obtained favored a mechanism that proceeded via the binding of an NO molecule to heme b_3 followed by hyponitrite bond formation via the binding of a second NO in a free form. N-O bond cleavage followed to yield N₂O and an oxo-bound non-heme center and was suggested as the rate limiting step as evident from an activation barrier of almost 22.6 kcal/mol – the highest calculated in the course of the reaction. The dinitrosyl (trans) mechanism was also explored but found unfavorable due to high energy barriers of the resulting intermediates.[12]

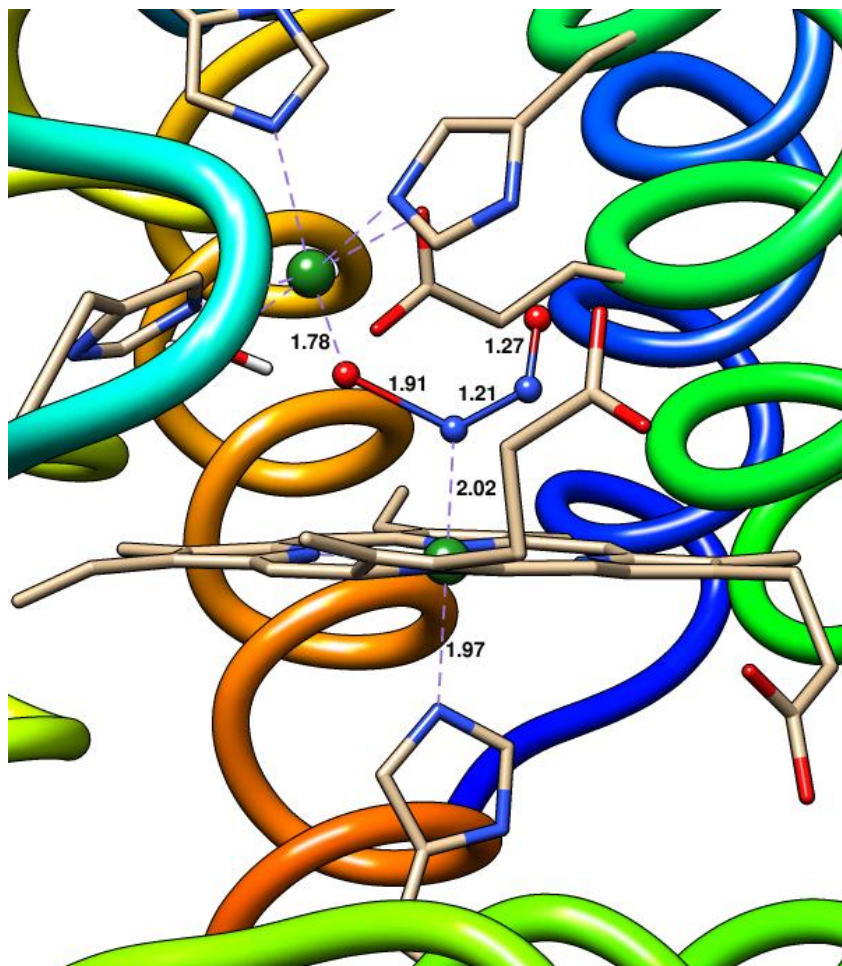


Figure 6.2. The optimized transition state for N-O bond cleavage and N_2O formation. Bond distances are in shown in Å.

Chapter 7. Assymetry within the $\text{Fe}(\text{NO})_2$ moiety of dithiolate dinitrosyl iron complexes.

The asymmetric behavior within iron dithiolate dinitrosyl models in $\{\text{Fe}(\text{NO})_2\}$ ⁷, $\{\text{Fe}(\text{NO})_2\}$ ⁸, $\{\text{Fe}(\text{NO})_2\}$ ⁹ and $\{\text{Fe}(\text{NO})_2\}$ ¹⁰ in addition to the relation between this asymmetry and the NO donation activity of DNICs were addressed in chapter 7. These phenomena of structural and geometrical asymmetries were made apparent by means of DFT, CASSCF calculations, *ab initio* MD simulations, as well as in reaction pathways

connecting the dinitrosyl state to a putative hyponitrite adduct. Such results confirmed the strong potential of DNICs to serve as nitric oxide donors and further provide insight into the mechanism of nitric oxide reduction by heme nitric oxide reductases through the critical step of N-N formation and the liberation of the stable N_2O moiety.[13]

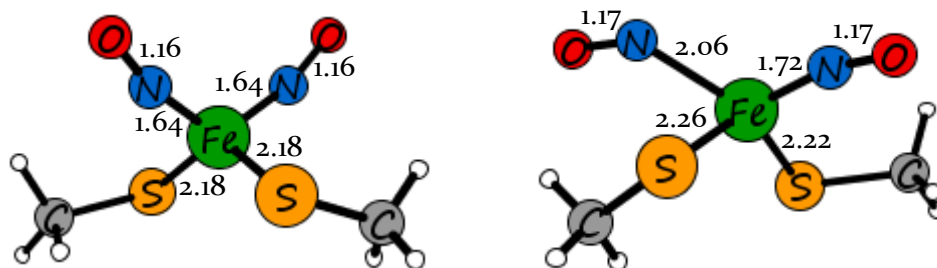


Figure 7.1. Optimized structures of the $\{Fe(NO)_2\}^8$ model in the $S=0$ (left) and $S=2$ (right) spin states.

Chapter 8. A theoretical study on the reaction pathways of peroxyxynitrite formation and decay at *non*-heme iron centers.

The third and final part of the thesis included two chapters that concerned the catalysis of nitrogen oxanions. In chapter 8, a density functional study was carried out to investigate the formation and decomposition of possible peroxyxynitrite isomers at *non*-heme models of the active sites of SOR and FeSOD in their ferrous and ferric oxidation states. The $Fe-OONO^-$ and $Fe-N(O)OO^-$ isomers were examined in both the *cis* and *trans* forms. For the $Fe-OONO^-$ isomer, the instant heterolytic cleavage of the O-ONO bond of all *cis* and *trans* ferrous complexes was noted whereas the *cis* and *trans* ferric adducts were found relatively stable with the *cis* isomers being energetically more favorable than their *trans* counterparts. The O-ONO bond cleavage in the *cis* and *trans* ferric adducts of the $Fe-OONO^-$ isomer was found to be energetically facile proceeding homolytically to yield nitrogen dioxide species for all models. [14]

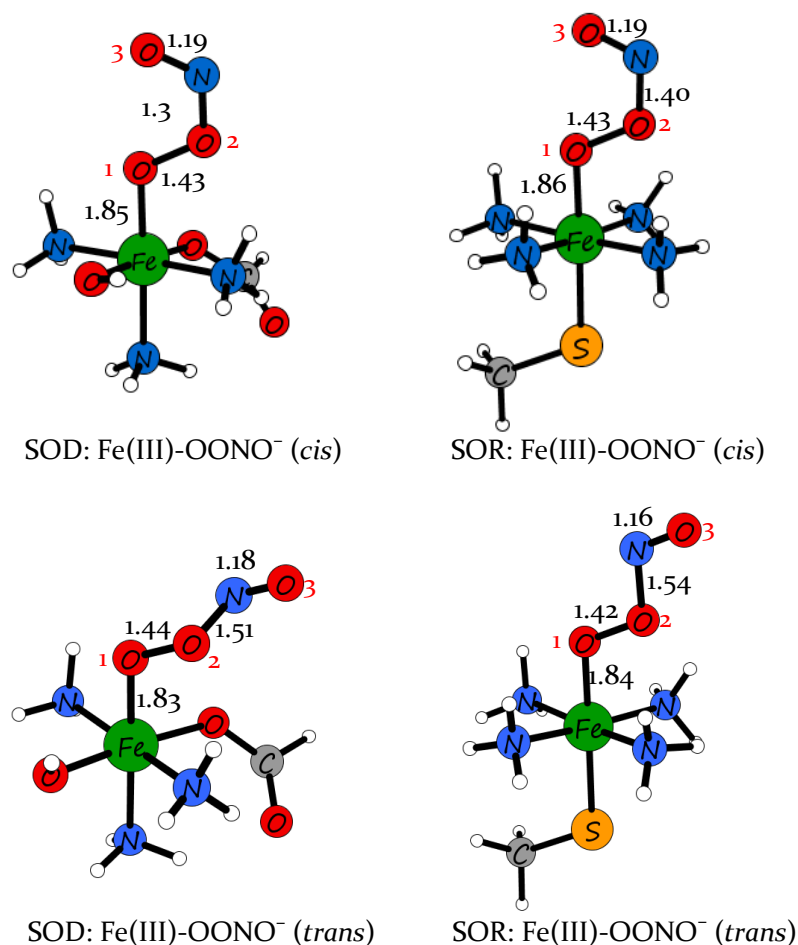


Figure 8.1. Geometry-optimized ferric OONO⁻ SOR and FeSOD adducts. Bond lengths are in (Å).

The active site models of FeSOD and SOR were shown to be only capable of accommodating the *cis* isomer of Fe-N(O)OO⁻. Overall, the ferric adducts of *cis* Fe-OONO⁻ isomer were found to be energetically more favorable than their Fe-N(O)OO⁻ counterparts and similarly, the protonated forms of all adducts of the Fe-OONOH isomer were found to be lower in energy than their equivalent Fe-N(O)OOH adducts. The energy costs for the decomposition of peroxyxynitrite were identified based on multiple suggested pathways and were found to depend on the peroxyxynitrite isomer, the type of model (whether an SOR or FeSOD active site) and the oxidation state of iron. [14]

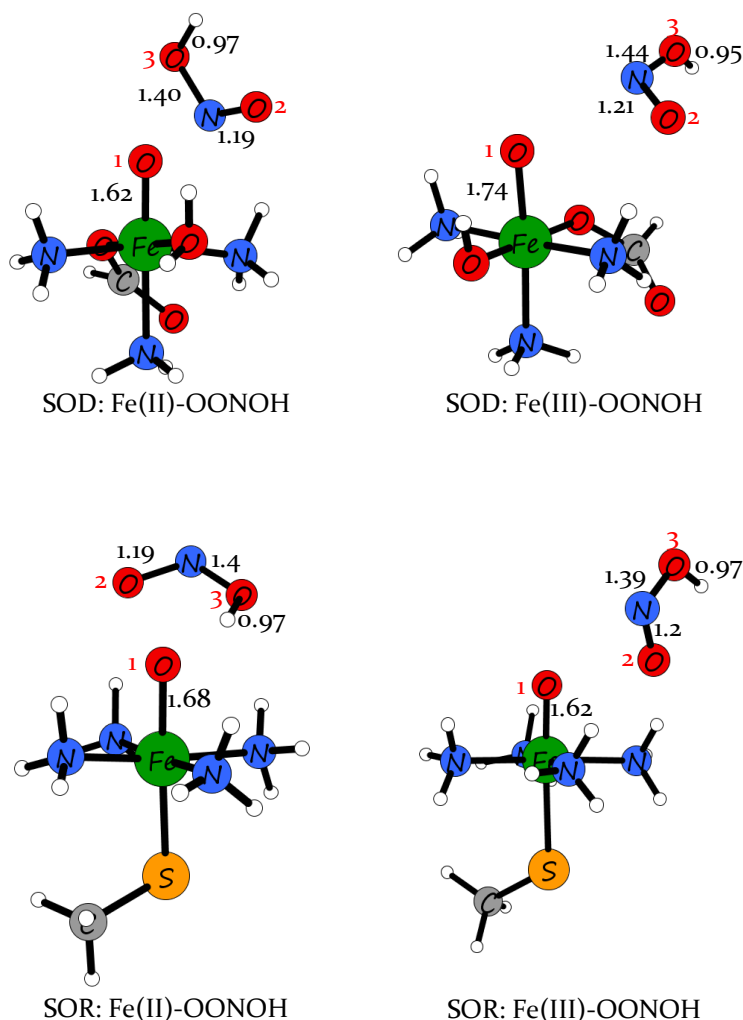


Figure 8.2. Geometry-optimized structures of the Fe-OONOH isomer. Bond distances are in (Å).

Chapter 9. Computational investigation of the initial two-electron, two-proton steps in the reaction mechanism of hydroxylamine oxidoreductase.

Last but not least, chapter 9 introduced the first attempt to investigate the 2-electron 2-proton reaction of Fe(III)-H₂NOH to Fe(III)-HNO in the catalytic cycle of hydroxylamine oxidoreductase [15]. Two subsequent protonation events were proposed to initiate the process, of which the second is suggested to be concerted with a one-electron

oxidation. The final one-electron oxidation is further proposed to be accompanied by a third deprotonation process, suggesting that Fe(III)-HNO may not be an isolable intermediate in the HAO catalytic cycle.

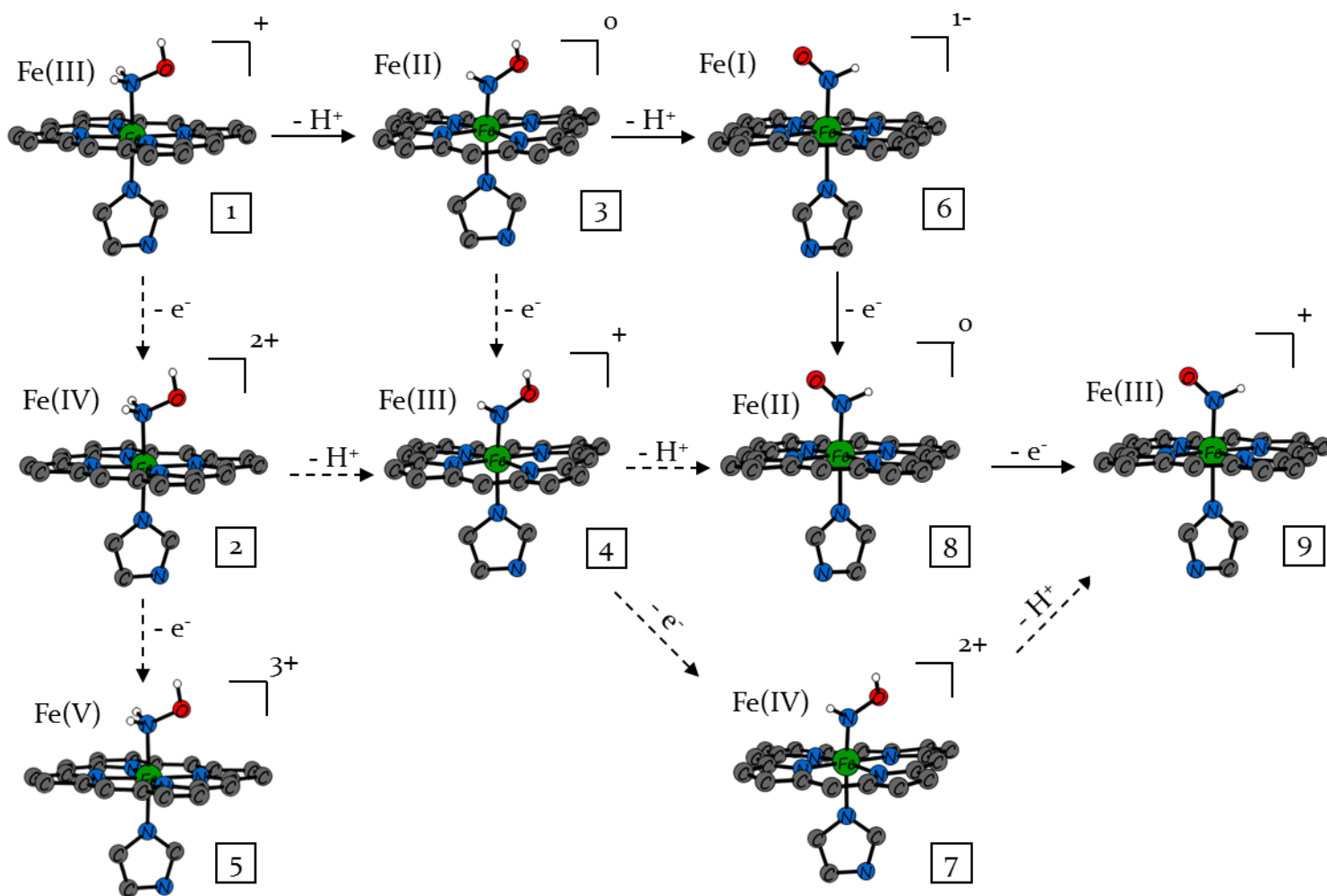


Figure 9.2. Proposed pathway for the 2-electron 2-proton transfer reaction of Fe(III)-H₂NOH to Fe(III)-HNO in HAO. Solid lines represent feasible pathways while dashed lines represent pathways that are highly unlikely to occur though not impossible. In each structure, hydrogen atoms of the porphine ring and the imidazole ligand are omitted for clarity.

Further explorations of the following steps in the catalytic cycle as well as the influence of the lateral substituents of the heme (and especially of the Cys and Tyr crosslinks) and the proton delivery network in the distal site on the mechanism were advocated.

References.

- [1] Amr A. A. Attia, D. Cioloboc, A. Lupan, R. Silaghi-Dumitrescu, *J. Biol. Inorg. Chem* 2013, 18, 95.
- [2] D. M. Kurtz Jr, *Acc Chem Res* 2004, 37, 902.
- [3] F. Aquilante, T. B. Pedersen, A. Sanches de Meras, H. Koch, *J Chem Phys* 2006, 125, 174101.
- [4] Amr A. A. Attia, A. Lupan, R. Silaghi-Dumitrescu, *RSC Adv* 2013, 3, 26194.
- [5] W. Nam, *Acc. Chem. Res.* 2007, 40, 522.
- [6] D. M. Kurtz, Jr. "Dioxygen-binding Proteins" in *Comprehensive Coordination Chemistry II* 2003, Volume 8, Pages 229-260
- [7] S. P. Visser *Coord. Chem. Rev.* 2009, 253, 754.
- [8] J. G. McCoy, L. J. Bailey, E. Bitto, C. A. Bingman, D. J. Aceti, B. G. Fox, G. N. Phillips Jr. *Proc Natl Acad Sci* 2006, 103, 3084.
- [9] D. M. Kurtz Jr, *Dalton Trans.* 2007, 4115.
- [10] R. Silaghi-Dumitrescu, D. M. Kurtz Jr., L. G. Ljungdahl, W. N. Lanzilotta, *Biochemistry* 2005, 44, 6492.
- [11] I. M. Wasser, S. de Vries, P. Meonne-Loccoz, I. Schroder, K. D. Karlin *Chem. Rev.*, 2002, 102, 1201.
- [12] M. R. A. Blomberg, P. E. M. Siegbahn, *Biochemistry* 2012, 51, 5173.
- [13] Amr A. A. Attia, Sergei Makarov, Anatoly Vanin, Radu Silaghi-Dumitrescu, *Inorg. Chim. Acta* 2014, 418, 42.
- [14] Amr A. A. Attia, Radu Silaghi-Dumitrescu, *Int. J. Quantum Chem.* 2014, 114, 652.
- [15] M. L. Fernandez, D. A. Estrin, S. A. Bari, *J. Inorg. Biochem.* 2008, 102, 1523.